Supplementary Information

Formation of a Bi-rhodium Boron Tube Rh_2B_{18} and Its Great CO_2 Capture Ability

Hung Tan Pham[#] and Minh Tho Nguyen[&,≠,§,*]

[&] *Computational Chemistry Research Group, Ton Duc Thang University, Ho Chi Minh City, Vietnam*

[≠] *Faculty of Applied Sciences, Ton Duc Thang University, Ho Chi Minh City, Vietnam*

[#] *Institute for Computational Science and Technology (ICST), Ho Chi Minh City, Vietnam*

[§] *Department of Chemistry, KU Leuven, Celestijnenlaan 200F, B-3001 Leuven, Belgium*

Email: nguyenminhtho@tdt.edu.vn; minh.nguyen@kuleuven.be

Table S1a. Electron density (ρ) and Laplacian ($\nabla^2\rho$) calculated for bond critical point (BCP), ring critical point (RCP) containing three centers of Rh_2B_{18} double ring structure.

RCP	ρ	$\nabla^2\rho$	BCP	ρ	$\nabla^2\rho$
			Rh19 Rh20	0.071	0.10
B1 B2 Rh19 B2 B3 Rh19 B3 B4 Rh19 B4 B17 Rh19 B7 B8 Rh19 B5 B17 Rh19 B5 B6 Rh19 B1 B8 Rh19 B6 B7 Rh19 B9 B10 Rh20 B10 B11 Rh20 B11 B18 Rh20 B12 B18 Rh20 B12 B13 Rh20 B15 B16 Rh20 B13 B14 Rh20 B9 B16 Rh20 B14 B15 Rh20	0.063	0.082	Rh19 B5 Rh19 B4 Rh19 B2 Rh19 B2 Rh19 B17 Rh19 B3 Rh19 B8 Rh19 B6 Rh19 B1 Rh19 B7 Rh20 B18 Rh20 B15 Rh20 B9 Rh20 B14 Rh20 B16 Rh20 B13 Rh20 B10 Rh20 B10 Rh20 B12 Rh20 B11	0.063	0.077

Table S1a. Electron density (ρ) and Laplacian ($\nabla^2\rho$) calculated for ring critical point (RCP) containing five centers and cage critical point (CRP) of Rh_2B_{18} double ring structure.

RCP	ρ	$\nabla^2\rho$
B1 B9 B16 Rh20 Rh19 B3 B10 B11 Rh20 Rh19 B3 B4 B11 Rh20 Rh19 B5 B12 B17 Rh19 Rh20 B6 B7 B14 Rh20 Rh19 B7 B14 B15 Rh20 Rh19	0.03	0.086
CCP	Density	Laplacian
B3 B11 Rh20 Rh19 B7 B14 Rh20 Rh19	0.030	0.086

Table 2. Cartesian Coordinates of Rh_2B_{18} and Rh_2B_{18}-$(CO_2)x$ with x = 1,2 and 3 (angstrom).

Structures	Cartersian Coordinate			
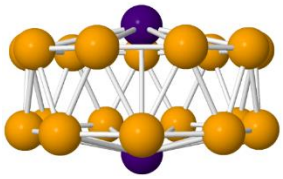 **18.A**	B	0.00000000	2.32570515	0.78392657
	B	-1.49493445	1.78159350	0.78392657
	B	-2.29037246	0.40385446	0.78392657
	B	-2.01411974	-1.16285257	0.78392657
	B	0.79543801	-2.18544796	0.78392657
	B	2.01411974	-1.16285257	0.78392657
	B	2.29037246	0.40385446	0.78392657
	B	1.49493445	1.78159350	0.78392657
	B	-0.79543801	2.18544796	-0.78392657
	B	-2.01411974	1.16285257	-0.78392657
	B	-2.29037246	-0.40385446	-0.78392657
	B	-0.00000000	-2.32570515	-0.78392657
	B	1.49493445	-1.78159350	-0.78392657
	B	2.29037246	-0.40385446	-0.78392657
	B	2.01411974	1.16285257	-0.78392657
	B	0.79543801	2.18544796	-0.78392657
	B	-0.79543801	-2.18544796	0.78392657
	B	-1.49493445	-1.78159350	-0.78392657
	Rh	-0.00000000	-0.00000000	1.27408400
	Rh	-0.00000000	-0.00000000	-1.27408400
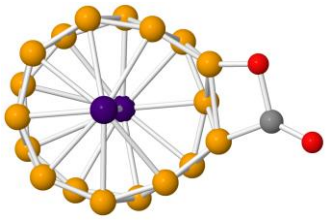 **1C.A**	B	2.83797800	-1.02583800	0.12430700
	B	2.97454800	0.57487800	0.09493500
	B	2.01934500	1.80343900	0.43424100
	B	0.54307700	2.28449900	0.87705700
	B	-1.45077200	0.21419800	1.44589000
	B	-1.07480000	-1.38391200	1.49018400
	B	0.17472300	-2.21931300	1.02891000
	B	1.69103900	-2.05254100	0.52833000
	B	2.45043100	-0.22327500	-1.38577000
	B	2.11911800	1.32529400	-1.26525600
	B	0.84303500	2.17631900	-0.87584700
	B	-2.00455000	1.12188100	0.01075900
	B	-2.19494500	-0.75402400	0.24586300
	B	-0.98917000	-1.77052100	-0.21129000
	B	0.43328200	-2.25860000	-0.74443500
	B	1.84292900	-1.67996100	-1.18509900
	B	-0.82602900	1.69918400	1.38885500
	B	-0.64873500	1.95691600	-0.36012200
	C	-3.66585200	-0.25108900	-0.17957000
	O	-4.74661600	-0.71305400	-0.37510900
	O	-3.36522500	1.11968200	-0.37874500
	Rh	0.22779400	-0.02312200	-1.25814200
	Rh	0.73192400	0.00779700	1.23371200
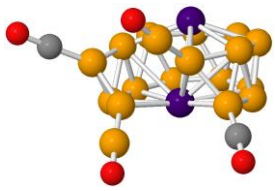 2C.A	B	-3.17377000	-1.06050500	-0.22033000
	B	-1.89814800	-2.00765400	-0.46894900
	B	-0.29970600	-2.03615300	-0.36482200
	B	1.38760000	-2.02801000	-0.37867800
	B	0.75690400	0.68016000	1.09288800
	B	-0.62766700	1.51079100	1.48187400
	B	-2.18001200	1.42918600	1.17910500
	B	-3.15064000	0.37240700	0.49298800
	B	-2.46775200	-0.91189700	-1.78562000

	B	-0.95992900	-1.43509700	-1.92616400
	B	0.60457000	-1.35883400	-1.73059200
	B	3.17482200	0.34540700	-1.16077100
	B	0.44674000	2.20190000	0.29274800
	B	-1.18717700	2.28314400	-0.02682100
	B	-2.54235100	1.65307800	-0.58872900
	B	-3.26995500	0.34779000	-1.23280500
	B	2.02595200	0.02125100	1.88631900
	B	1.79194500	-0.48638200	-0.87097700
	C	1.52659900	3.21690100	0.24756700
	C	2.40635700	-3.04782500	-0.05670100
	O	2.40820200	3.93704100	0.18083800
	O	4.15300800	1.02908600	-1.38210400
	O	2.92181000	-0.47910000	2.53824500
	O	3.24271000	-3.74494400	0.28744100
	Rh	-0.17335000	0.49096200	-0.92270300
	Rh	-1.32799900	-0.59216300	1.08950600
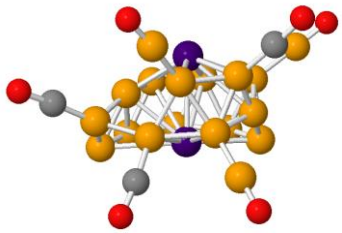 3C.A	B	2.08863500	-2.11375300	1.04399600
	B	2.10290400	-0.71174500	1.81193100
	B	1.50772000	0.52763900	1.07471100
	B	-0.29232300	1.12776300	1.20463500
	B	-1.75048000	0.24609000	0.50541600
	B	-2.00210600	-2.33421100	-0.01061100
	B	-0.60005700	-3.04165900	-0.12453900
	B	1.00395400	-3.01691400	0.23884700
	B	2.74534900	-0.60668300	0.08853000
	B	4.25354400	-0.02944700	-0.25634800
	B	0.87597300	1.67990000	0.02399200
	B	-1.56774900	2.29205400	-1.56682300
	B	-2.49377300	-0.92482500	-0.62189500
	B	-0.92494500	-1.45068600	-1.09080300
	B	0.49424700	-2.26264300	-1.22614700
	B	1.92900300	-1.82860500	-0.67236300
	B	-0.61149400	1.88022300	2.64530200
	B	-0.74534500	1.38800000	-0.47850300
	C	-3.63343900	-0.58112200	-1.52060000
	C	1.59742300	2.94510000	-0.26269200
	C	-2.85676200	0.44119700	1.49932700
	O	-4.53359100	-0.29608200	-2.15598500
	O	-2.21998400	2.86962500	-2.41294700
	O	5.33477200	0.44700500	-0.53165200
	O	2.18905400	3.88221000	-0.52841900
	O	-0.88169500	2.42189800	3.69439200
	O	-3.76094500	0.50714900	2.19510300
	Rh	0.70086800	-0.05248500	-1.24938700
	Rh	-0.02819100	-1.04947000	0.95323700

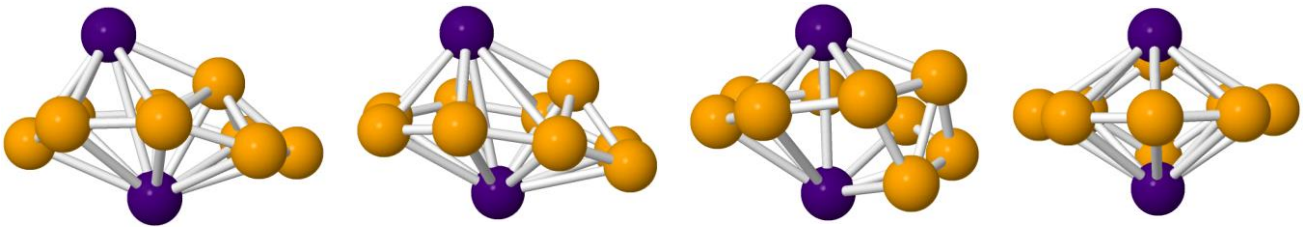

9.A C_s $^1A'$ 0.0 C_s $^3A''$ 7.4

9.B C_s $^1A'$ 2.0 C_s $^3A''$ 6.1

9.C C_1 ^1A 17.2 C_1 ^3A 6.8

9.D C_{2v} $^1A_1$ 20.0 C_{2v} $^3B_2$ 23.4

Figure S1. The lower-lying isomers of $Rh_2B_9^-$ clusters. Geometry optimization and energy calculations were performed by using the TPSSh functional combining with 6-311+g(d) basis set for B and aug-cc-pVTZ-PP for Rh.

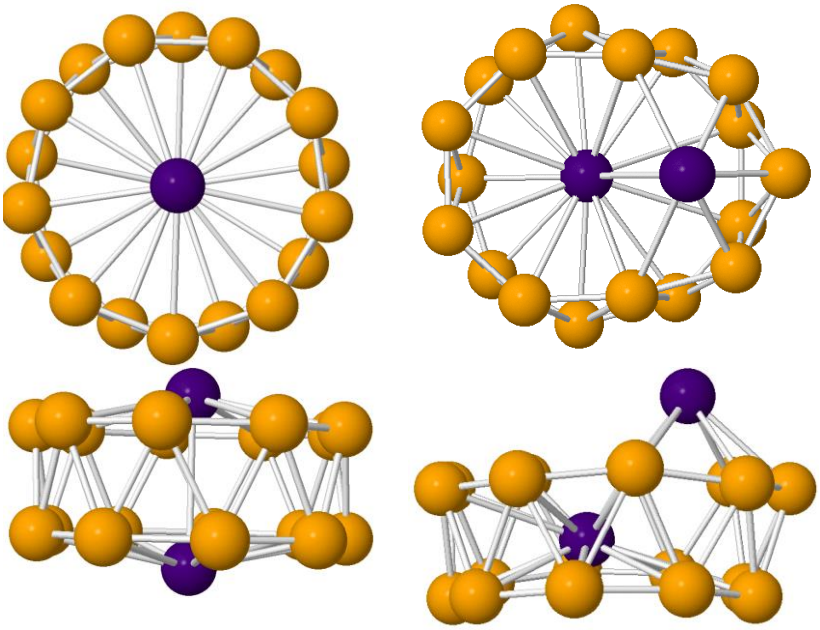

18.A $^1D_{9d}$ 0.0 $^3D_{9d}$ 34.0

18.B ^1C_s 35.0 ^3C_s 44.5

Figure S2. The shape and relative energy (kcal/mol) of lower-lying isomers of Rh2B18 cluster. Geometry optimization and energy calculations were performed by using the TPSSh functional combining with 6-311+g(d) basis set for B, C, O and aug-cc-pVTZ-PP for Rh.

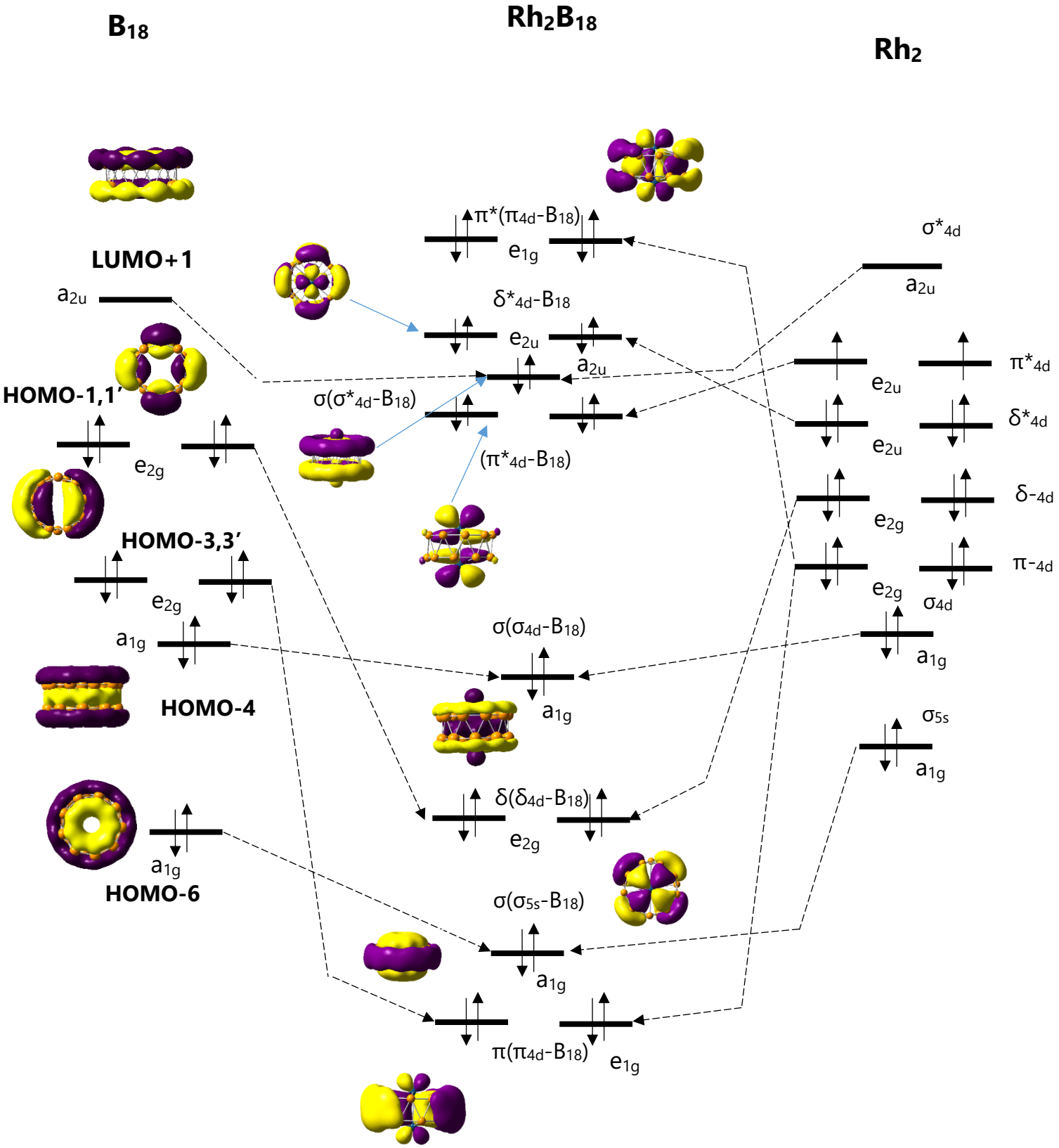
B18
Rh2B18
Rh2
LUMO+1
a2u
HOMO-1,1'
e2g
HOMO-3,3'
e2g
a1g
HOMO-4
a1g
HOMO-6
π*(π4d-B18)
e1g
δ*4d-B18
e2u
a2u
σ(σ*4d-B18)
(π*4d-B18)
σ(σ4d-B18)
a1g
δ(δ4d-B18)
e2g
σ(σ5s-B18)
a1g
π(π4d-B18)
e1g
σ*4d
a2u
e2u
π*4d
e2u
δ*4d
e2g
δ-4d
e2g
π-4d
σ4d
a1g
σ5s
a1g

Figure S3. The qualitative presence of orbital interaction between B_{18} tube and Rh_2 resulting Rh2B18 cluster.

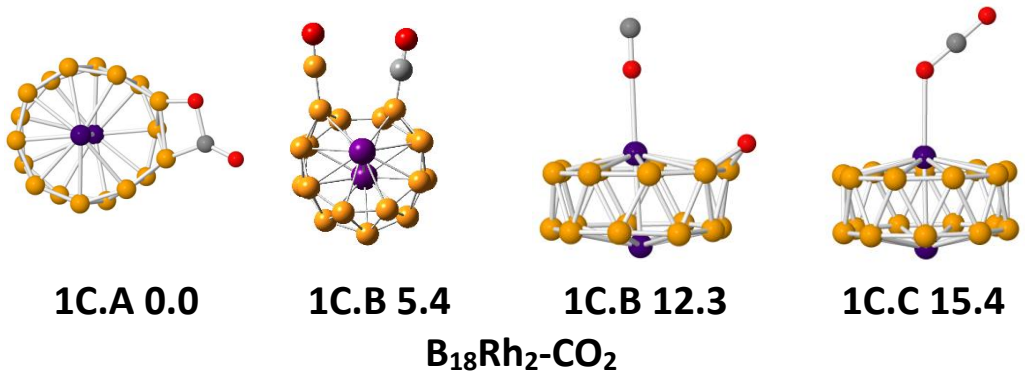

Figure S4. The shape and relative energy of configuration of Rh_2B_{18}-CO_2. Geometry optimization and energy calculations were performed by using the TPSSh functional combining with 6-311+g(d) basis set for B, C, O and aug-cc-pVTZ-PP for Rh.

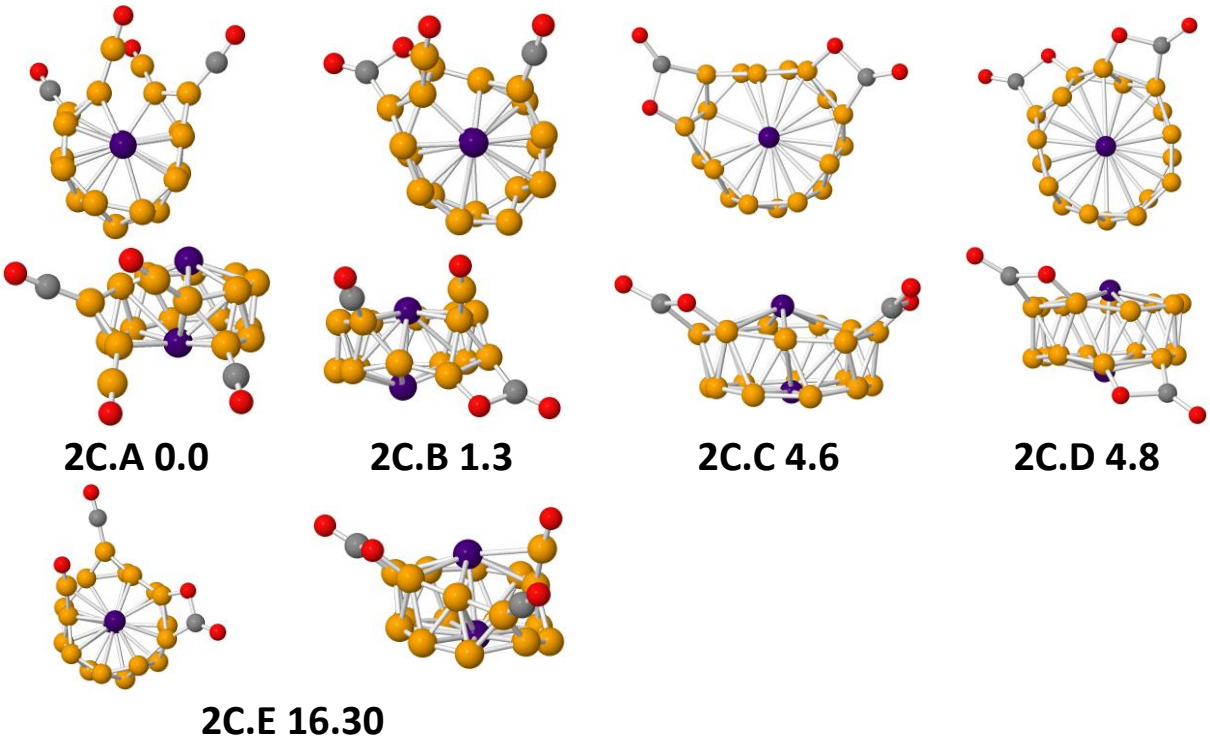

Figure S5. The shape and relative energy of configuration of Rh_2B_{18}-$(CO_2)_2$. Geometry optimization and energy calculations were performed by using the TPSSh functional combining with 6-311+g(d) basis set for B, C, O and aug-cc-pVTZ-PP for Rh.

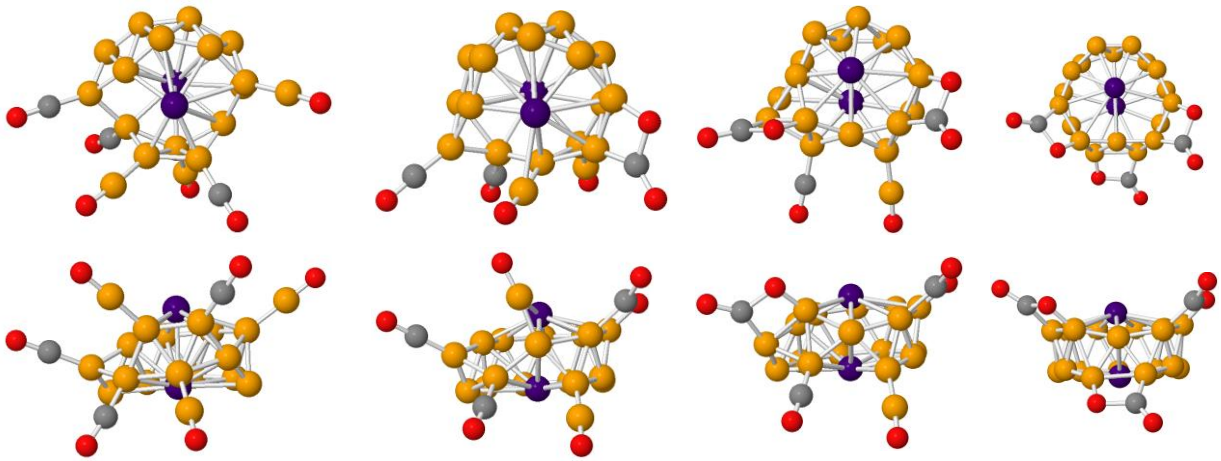

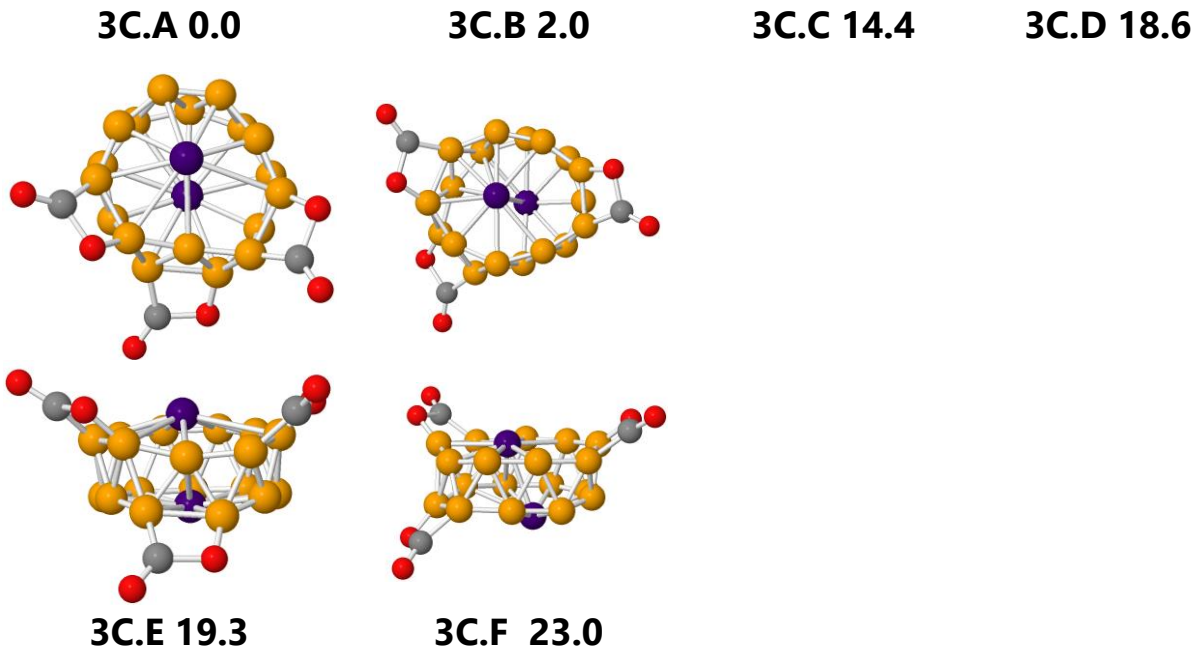

Figure S6. The shape and relative energy of configuration of Rh_2B_{18}-$(CO_2)_3$. Geometry optimization and energy calculations were performed by using the TPSSh functional combining with 6-311+g(d) basis set for B, C, O and aug-cc-pVTZ-PP for Rh.

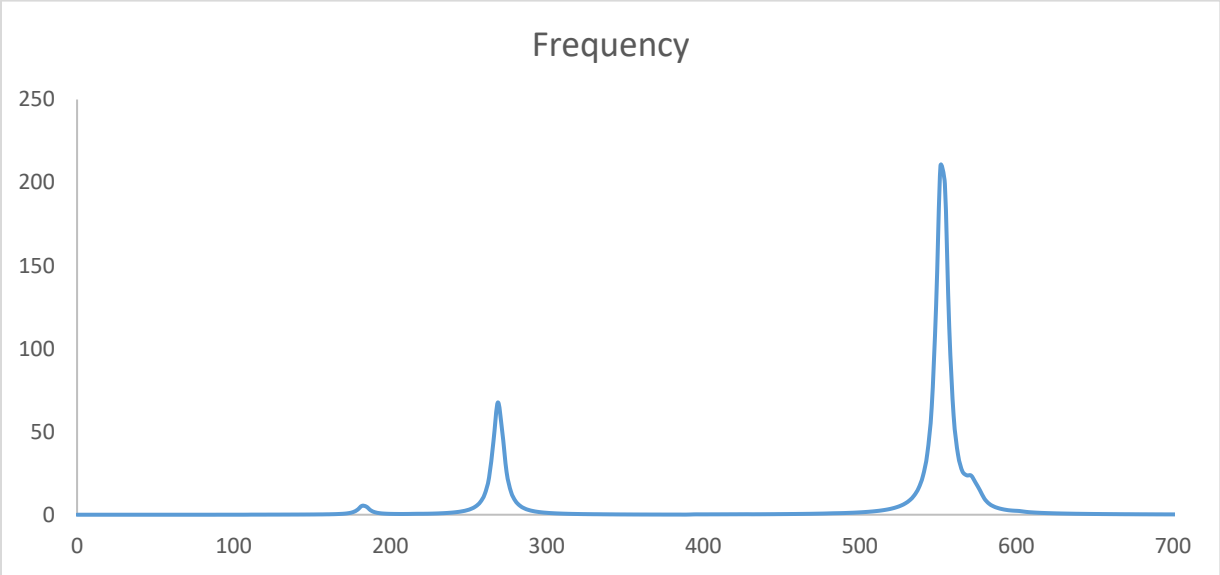

Figure S7. The IR spectrum of 18.A. The frequeny calculations were performed by using the TPSSh functional combining with 6-311+g(d) basis set for B, C, O and aug-cc-pVTZ-PP for Rh.

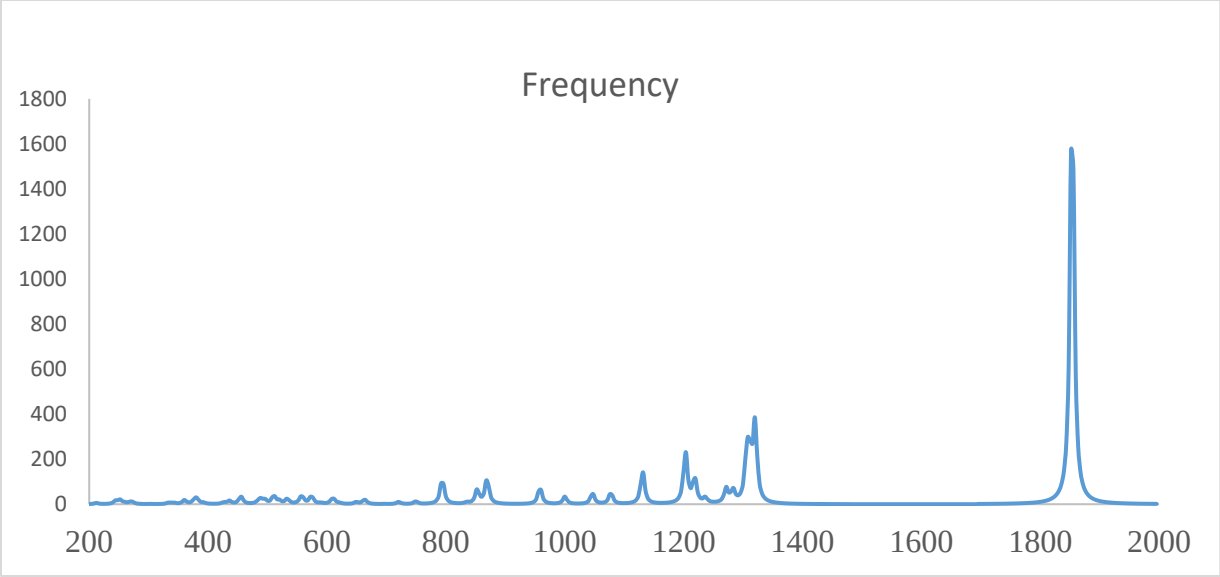

Figure S8. The IR spectrum of 1C.A. The frequeny calculations were performed by using the TPSSh functional combining with 6-311+g(d) basis set for B, C, O and aug-cc-pVTZ-PP for Rh.

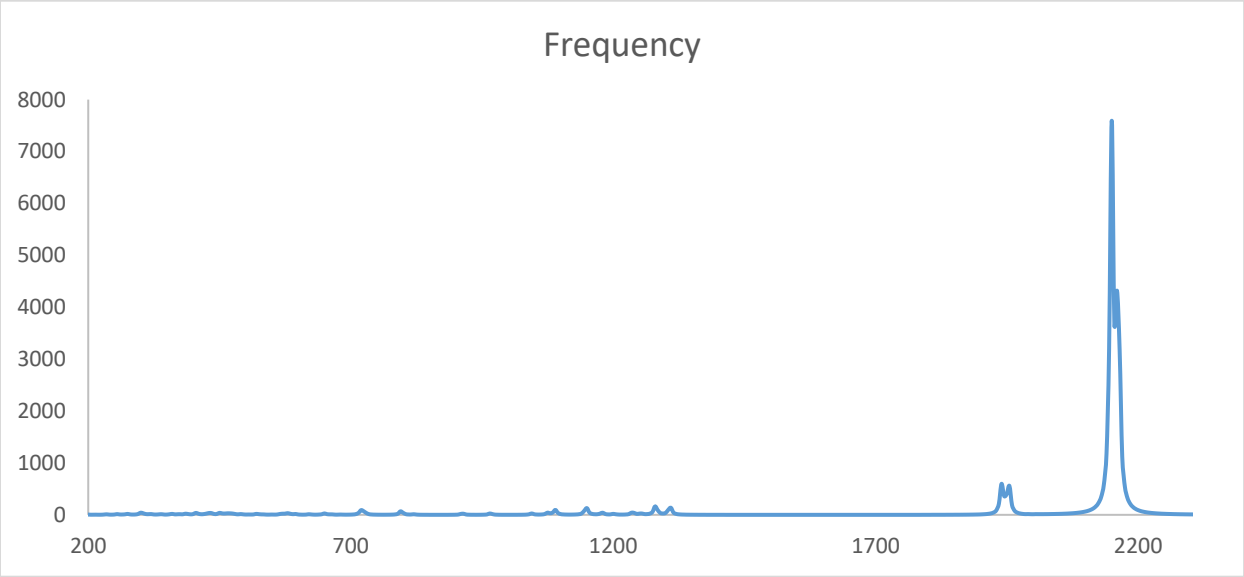

Figure S9. The IR spectrum of 2C.A. The frequeny calculations were performed by using the TPSSh functional combining with 6-311+g(d) basis set for B, C, O and aug-cc-pVTZ-PP for Rh.

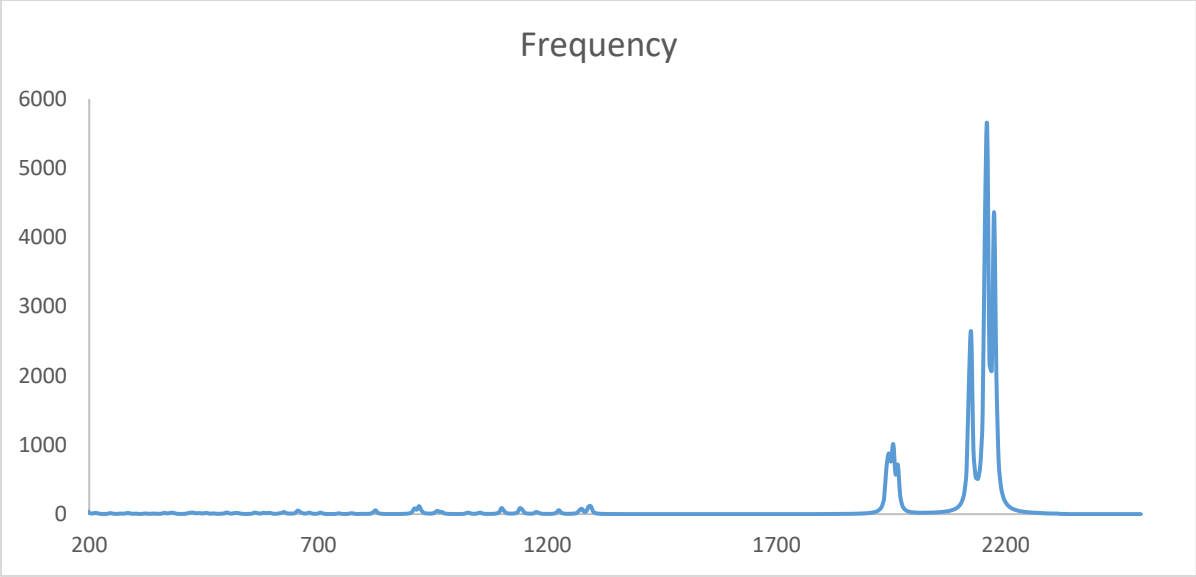

Figure S10. The IR spectrum of 3C.A. The frequeny calculations were performed by using the TPSSh functional combining with 6-311+g(d) basis set for B, C, O and aug-cc-pVTZ-PP for Rh.

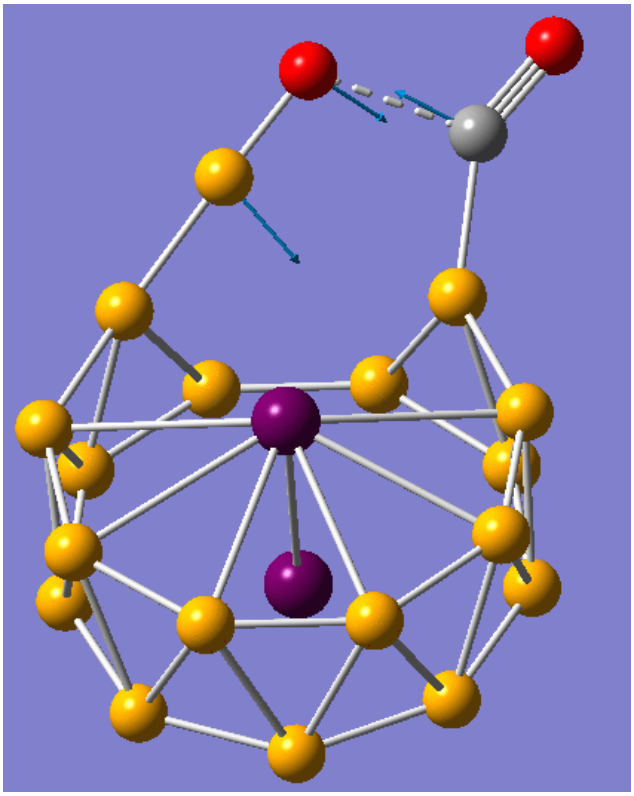

Figure S11. Reaction mode of transition structure 1C.TS

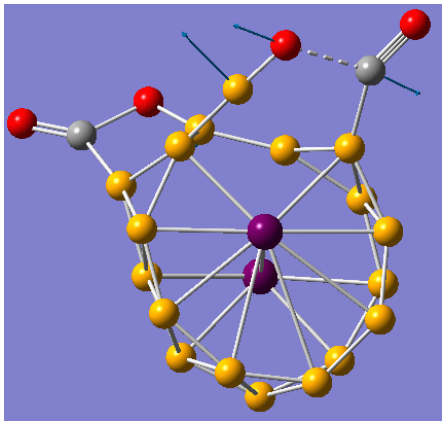

2C.D.TS1

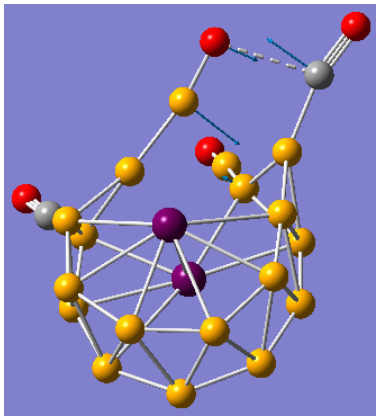

2C.D.TS2

a)

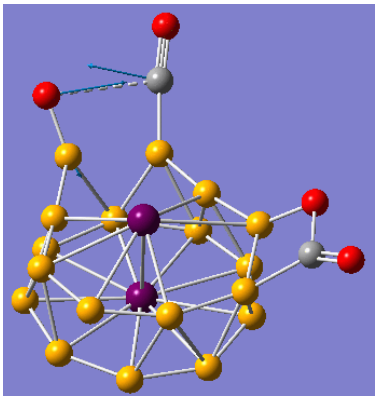

2C.C.TS1

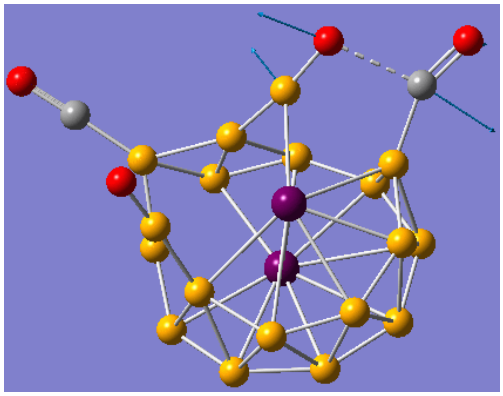

2C.C.TS2

b)

Figure S12. Reaction mode of a) **2C.D.TS1**, **2C.D.TS2** and b) **2C.C.TS1** and **2C.C.TS2**.

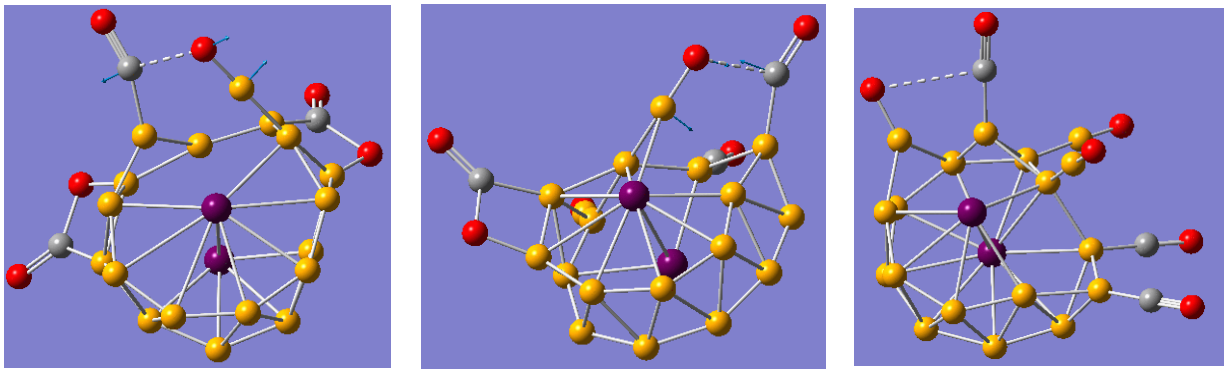

3C.TS1 **3C.TS2** **3C.TS3**

Figure S13. Reaction mode of **3C.TS1**, **3C.TS2** and **3C.TS3**

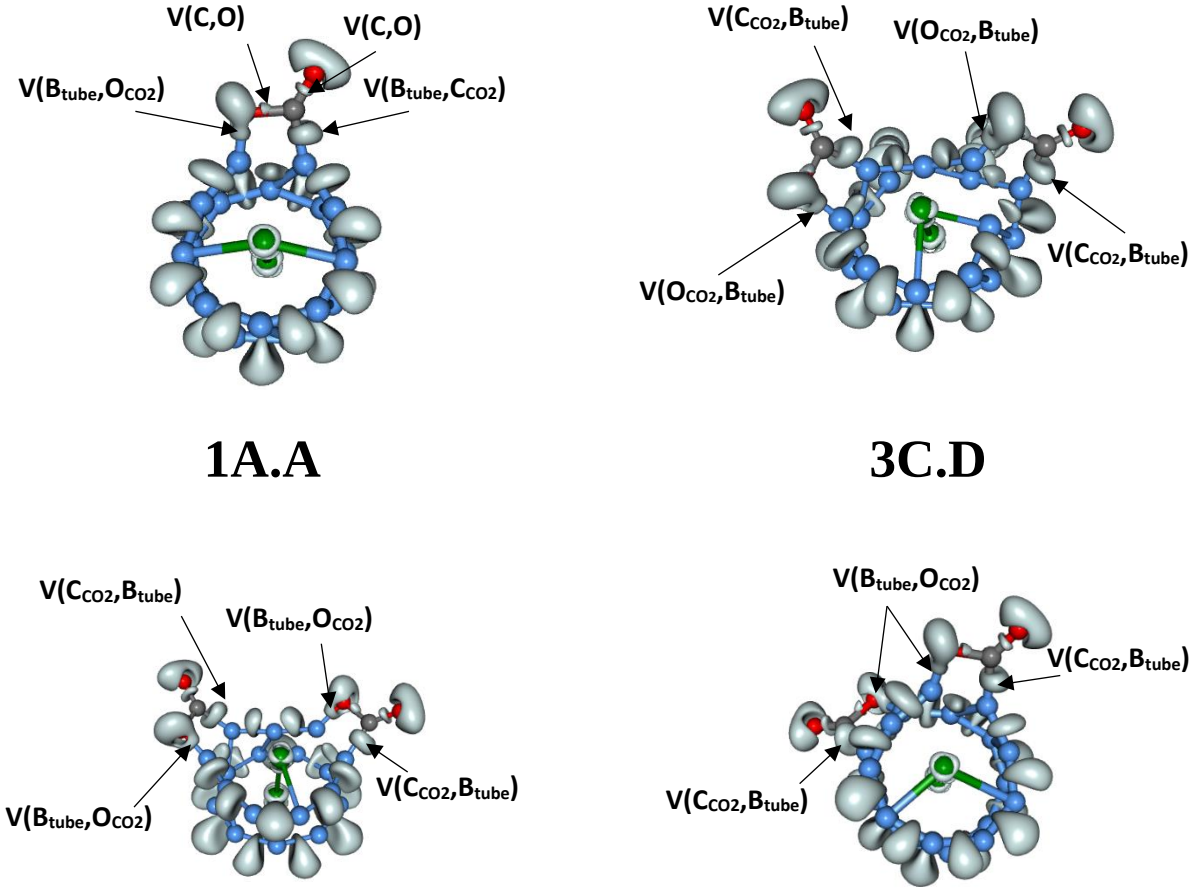

2C.C

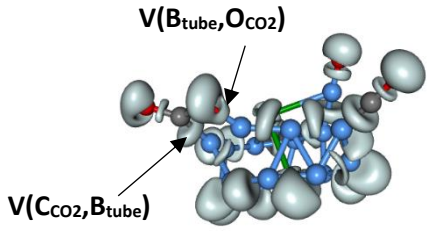

2C.D

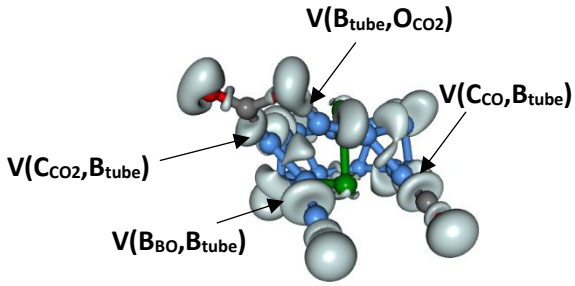

2C.E

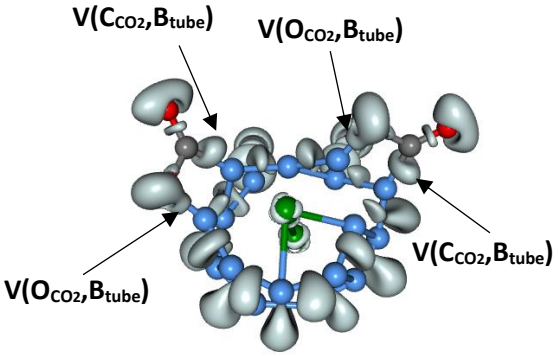

2C.B

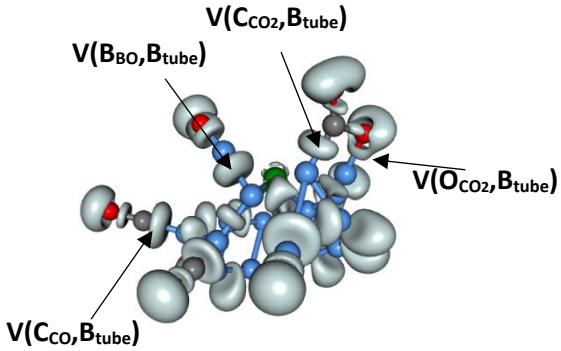

3C.D

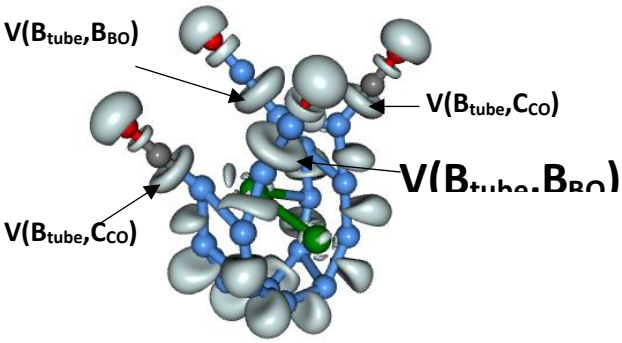

3C.B

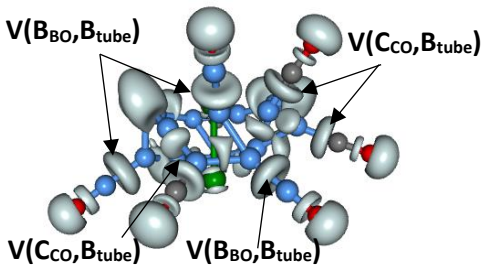

2C.A

3C.A

Figure S14. The ELI_D surface maps plotted at the bifurcation value of 1.45 for **1C.A, 2C.A, 2C.C,2C.D, 2C.E, 3C.A, 3C.B, 3C.A.**